RSC Advances

ROYAL SOCIETY OF CHEMISTRY

www.rsc.org/advances

Journal Name

RSCPublishing

ARTICLE

Two novel 3D lanthanide supramolecular coordination polymers constructed by paddle wheel SBUs and hydrogen bonding: synthesis, structures and properties

Cite this: DOI: 10.1039/x0xx00000x

Received 00th January 2012,
Accepted 00th January 2012

DOI: 10.1039/x0xx00000x

www.rsc.org/

Qipeng Li,[a,b] and Shaowu Du*[a]

Two novel 3D lanthanide supramolecular coordination polymers, formulated as {[$Ln_2(PIP)_2(HPIP)(HCO_2)(H_2O)_2$]·$H_2O$} (Ln = Tb **1**, Eu **2** and H_2PIP = 5-(pyridine-4-yl)isophthalic acid) have been solvothermally synthesized through *in situ* generation of formate anion. Single-crystal X-ray diffraction studies reveal that they are isomorphic and both display a 2D layered structure constructed by lanthanide paddle wheel SBUs and expanded by hydrogen bond interactions into a 3D-supramolecular architecture. Temperature dependent luminescent measurements show that compounds **1** and **2** exhibit bright green and red fluorescence at 10 K with long lifetimes of 1.00 and 1.19 ms and moderate quantum yields of 44.66% (at 310 nm) and 26.75% (at 338 nm), respectively. In addition, an anti-ferromagnetic interaction between the Tb(III) ions is observed in **1**.

Introduction

Lanthanide coordination polymers (Ln-Cps) have been receiving extensive and enduring research interest not only due to their unique optical and magnetic properties but also but also because of their potential applications in lighting, display, sensing, optical devices[1] and molecule-based magnetic materials.[2] Such Ln-Cps can be readily self-assembled by combining lanthanide ions with various organic linkers under solvothermal conditions.[3] However, compared to the d-block transition metals, the use of lanthanide ions as nodes in the construction of Cps is still less developed. This is because that the high coordination number and flexible coordination geometry of lanthanide ions may cause difficulty in controlling the synthetic reactions and thereby the structures of the products.[4] Therefore, selection of suitable organic ligands with certain features is crucial in the building of Ln-Cps. Recently, some studies of pyridine-3,5-dicarboxylic acid (3,5-H_2PDC) have been drawn attention to assemble with lanthanide ions to construct Ln-Cps with luminescent and magnetic properties.[5] By comparison, Ln-Cps built up from 5-(4-pyridyl) isophthalic acid (H_2PIP), which has one additional benzene ring compared to 3,5-H_2PDC (Scheme 1), has less reported.[6] It is anticipated that the increase of π-conjugation system in H_2PIP might contribute much to the large diversity of supramolecular architectures and the desirable fluorescence properties of the products.

On the other hand, in addition to organic ligands, the solvents used in solvothermal synthesis are also considered an important factor in controlling the assembly of Ln-Cps because they have effects on the control of kinetic or thermodynamic conformers as well as the coordination modes of the ligands.[7] In some cases, *in situ* generation of ligands can occur by the decomposition of solvents. For example, it has been documented that the *in situ* decomposition of DMSO and DMF at solvothermal conditions generated sulfate and formate anions, respectively, which subsequently serve as auxiliary ligands for the construction of Ln-Cps.[8, 9]

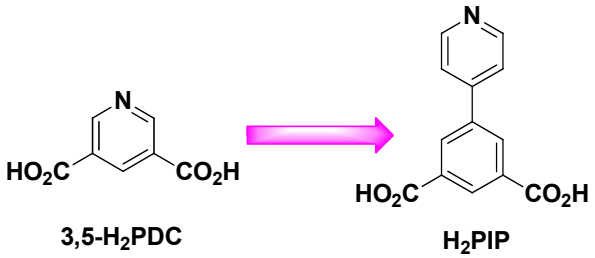

Scheme 1 Structures of 3,5-H_2PDC (left) and H_2PIP (right) ligands.

In our present study, we employed H_2PIP to synthesize two novel Ln-Cps, {[$Ln_2(PIP)_2(HPIP)(HCO_2)(H_2O)_2$]·$H_2O$} (Ln = Tb **1** and Eu **2**) via *in situ* generation of formate anion under solvothermal conditions. Significantly, they both contain a lanthanide paddle wheel SBU, which is common in transition

metal Cps, but is not the same for Ln-Cps.[4, 10] The temperature dependent luminescent properties of them have also been studied, and the results show that they exhibit bright green and red emissions at 10 K, respectively with long luminescence lifetimes and moderate luminescence quantum yields. Besides, variable-temperature magnetic susceptibility measurement of **1** reveals an anti-ferromagnetic interaction between the Tb(III) ions.

Experimental

Materials and methods

All the chemicals were purchased commercially and used as received. Thermogravimetric experiments were performed using a TGA/NETZSCH STA-449C instrument heated from 30−1000 ºC (heating rate of 10 ºC /min, nitrogen stream). IR spectra using KBr pellets were recorded on a Spectrum-One FT-IR spectrophotometer. The powder X-ray diffraction (XRD) patterns were recorded on crushed single crystals in the 2θ range 5−50º using Cu-Kα radiation. Fluorescence spectra of the solid samples were performed on an Edinburgh Analytical instrument FLS920. The magnetic susceptibility data was collected on Quantum Design MPMS (SQUID)-XL magnetometer.

Synthesis of $[Ln_2(PIP)_2(HPIP)(HCO_2)(H_2O)_2]\cdot H_2O$ (Ln = Tb 1 and Eu 2).

H_2PIP (0.50 mmol, 121 mg) and $Tb(NO_3)_3\cdot 6H_2O$ (0.25 mmol, 110 mg) were placed in a 20 mL of Teflon-lined stainless steel vessel with 6 mL mixed-solvent of DMF and CH_3CN (V / V = 1:1). The mixture was heated to 120 ºC in 4 h, kept at this temperature for 3 days and then cooled slowly to room temperature during another 2 days. Colourless crystals of **1** were collected and washed with DMF, and dried in air (50% yield based on $Tb(NO_3)_3.6H_2O$). Elemental anal. calcd. for **1** $Tb_2C_{40}H_{28}N_3O_{17}$ (1140.49): C, 42.12; H, 2.47; N, 3.68%. Found: C, 42.50; H, 2.51; N, 3.73%. IR (KBr, cm^{-1}): 3419 s, 2327 vw, 2025 w, 1659 s, 1443 m, 1384 m, 1106 vw, 831 vw, 780 m, 720 vw.

Colourless crystals of **2** were obtained in 45% yield by a similar method as described for **1** except that $Eu(NO_3)_3.6H_2O$ was used instead of $Tb(NO_3)_3.6H_2O$. Elemental anal. calcd. for **2** $Eu_2C_{40}H_{28}N_3O_{17}$ (1126.59): C, 42.65; H, 2.51; N, 3.73%. Found: C, 42.11; H, 2.46; N, 3.68%. IR (KBr, cm^{-1}): 3440 s, 2310 vw, 2045 w, 1642 s, 1440 m, 1389 m, 1195 vw, 828 vw, 785 m, 713 vw.

Crystal Structure Determination

Single-crystal X-ray diffraction data were collected on a Rigaku Diffractometer with a Mercury CCD area detector (Mo Kα; λ = 0.71073 Å) at room temperature. Empirical absorption corrections were applied to the data using the Crystal Clear program.[11] The structure was solved by the direct method and refined by the full-matrix least-squares on F^2 using the SHELXTL-97 program.[12] Metal atoms were located from the *E*-maps and other non-hydrogen atoms were located in successive difference Fourier syntheses. All non-hydrogen atoms were refined anisotropically. The organic hydrogen atoms were positioned geometrically, while those of the water molecules were located using the difference Fourier method and refined freely. The C atoms in pyridine ring are disordered equally over two positions. PLATON/SQUEEZE was employed to remove the heavily disordered water molecules and the final formula of **1** was calculated from the TGA result. Crystallographic data and other pertinent information for **1** are summarized in Table S1†. Selected bond distances and angles are listed in Table S2†. Bond lengths and angles of hydrogen bonds are listed in Table S3†. The CCDC number for **1** is 874175. For **2**, because single crystals suitable for X-ray diffraction were unable to obtained, only the lattice parameters were determined: a = 13.132, b = 13.874, c = 16.249 Å, α = 75.645, β = 66.386, γ = 82.451°, V = 2617.35 Å^3.

Results and Discussion

Synthesis and description of Crystal Structures

The solvothermal reaction of $Tb(NO_3)_3\cdot 6H_2O$ and H_2PIP ligand in a mixed-solvent of DMF and CH_3CN (V/V = 1:1) led to two novel Ln-Cps, formulated as $\{[Ln_2(PIP)_2(HPIP)(HCO_2)(H_2O)_2]\cdot H_2O\}$ (Ln = Tb **1** and Eu **2**) via *in situ* generation of formate. Compounds **1** and **2** are isomorphic, which is confirmed by PXRD, TGA, IR, elemental analysis and lattice parameters.

Compound **1** crystallizes in the triclinic space group *P*–1 and its asymmetric unit consists of two crystallographically independent Tb(III) ions, two PIP^{2-} ligands, one $HPIP^-$ ligand, one formate anion and two coordinated water molecules and one lattice water molecule. Each Tb(III) center is octa-coordinated by two carboxylate O atoms from two different $HPIP^-$ ligands, four carboxylate O atoms from three different PIP^{2-} ligands, one O atom from the coordinated water molecule and one carboxylate O atom from the formate anion (Fig. 1a). In **1**, the $HPIP^-$ ligand where the pyridyl group is protonated, as confirmed by the charge balance and bond valence sum calculations,[13] displays a $(\kappa^1\text{-}\kappa^1)\text{-}(\kappa^1\text{-}\kappa^1)\text{-}\mu_4$ coordination mode and acts as a countercation (Scheme 2, A), while the PIP^{2-} ligand adopts a $(\kappa^2)\text{-}(\kappa^1\text{-}\kappa^1)\text{-}\mu_3$ coordination mode (Scheme 2, B). Eight Tb(III) ions are bridged by the ligands to form a $[Tb_8(PIP)_2(HPIP)_2(HCO_2)]$ eight-membered ring, in which the aromatic rings of two $HPIP^-$ ligands are arranged in an offset face-to-face mode with the parallel distance of 3.4552(4) Å, indicating the existence of weak π-π stacking in the structure (Fig. 1b).

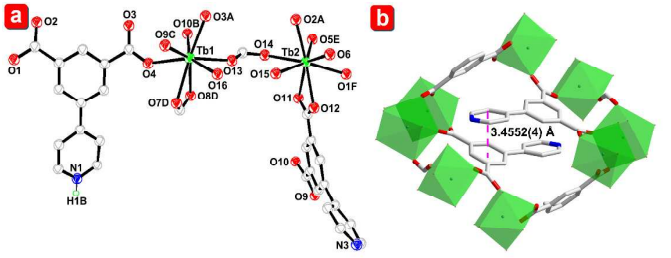

Fig. 1 (a) Representation of the coordination environment of the Tb1 and Tb2 ions in compound **1**. Symmetry codes: A −*x*+2, −*y*, −*z*; B −*x*+2, −*y*+1, −*z*; C *x*, *y*−1, *z*; D *x*+1, *y*, *z*; E −*x*+1, −*y*+1, −*z*; F *x*−1, *y*+1, *z*. (b) View of the π-π stacking interaction between aromatic rings of $HPIP^-$ ligands in **1**.

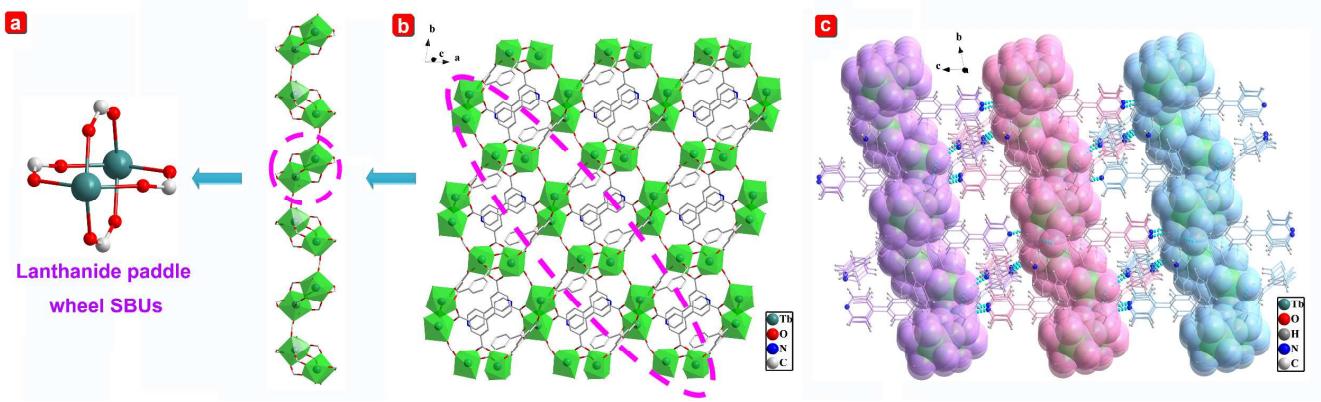

Fig. 2 (a) The lanthanide paddle wheel SBU and 1D lanthanide-carboxylate chain in **1**. (b) The 2D layer structure. **(c)** 3D supramolecular architecture.

In addition, two equivalent Tb(III) ions are bridged by four carboxyl groups in a *syn-syn* fashion to generate a lanthanide paddle wheel SBU $\{Tb_2(COO)_4\}$ (Fig. 2a), which forms a 1D chain through formate bridges. These chains are further extended into a 2D layer network via the carboxyl groups of ligands (Fig. 2b), which is stabilized by the intra-layer hydrogen bonds between the O atoms of coordinated water molecules and the O atoms of the formate anion (O15—H15···O13 = 2.750(4) Å, ∠O15—H15···O13 = 147°), and between the two coordinated water molecules (O15—H15···O16 = 3.283(4) Å, ∠O15 —H15···O16 = 138°) (Table S3†). Furthermore, there exist intermolecular hydrogen bonds between the O atoms of coordinated water molecules and the N atoms of PIP^{2-} ligands (O16—H16B···N2^{ii} = 2.875(5) Å, ∠O16—H16B···N2^{ii} = 171° and O15—H15A···N3^{i} = 2.752(5) Å, ∠O15—H15A···N3^{i} = 166°), and between the O atoms of coordinated water molecules and the N atoms of $HPIP^-$ ligands (N1—H1B···O16^{iii} = 2.788(4) Å and ∠N1—H1B···O16^{iii} = 138°), which expand the 2D layers into a 3D-supramolecular architecture (Fig. 2c).

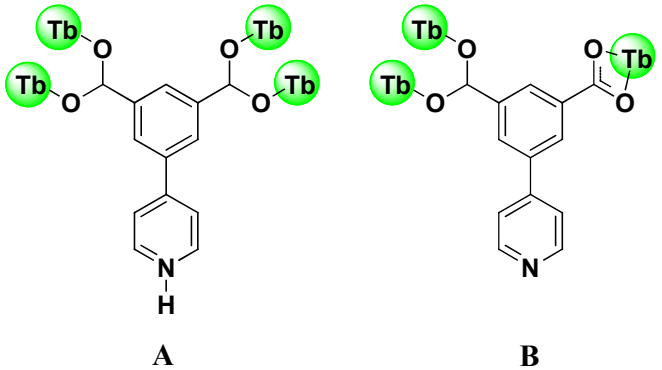

Scheme 2 The coordination modes of $HPIP^-$ (A) and PIP^{2-} (B) ligands in **1**.

XRD patterns and thermal properties

Powder X-ray diffraction (XRD) of **1** and **2** was performed to characterize their purity at room temperature (Fig. S1†). The experimental results match well with the simulated XRD patterns, indicating the phase purity of the as-synthesized samples. Thermogravimetric analysis (TGA) measurement was conducted to study the thermal stability of the compounds. The TGA curve of **1** indicates that the first weight loss of 1.60% from 40 to 150°C corresponds to the elimination of one lattice water molecule (calcd. 1.58%), and then it begins to decompose upon further heating. The TGA curve of **2** is very similar to that of **2** (Fig. S2†).

Luminescence properties

The luminescence properties of **1** and **2** were explored at 298, 77 and 10 K in the solid state, which emitted the intense bright green and red fluorescence under UV light, respectively. The free H_2PIP ligand presented an emission with the band peaking around 459 nm upon excitation at 394 nm (Fig. 3).

When excited at 310 nm, **1** exhibits bright green emission with typical emission peaks at 489, 543, 584 and 621 nm, which are assigned to $^5D_4 \rightarrow {}^7F_J$ (J = 6-3) transitions. The strong luminescent emission band at 543 nm arises from the $^5D_4 \rightarrow {}^7F_5$ transition and the less strong band at 489 nm is attributed to the $^5D_4 \rightarrow {}^7F_6$ transition. The other weaker emission bands at 584 and 621 nm correspond to the $^5D_4 \rightarrow {}^7F_4$ and $^5D_4 \rightarrow {}^7F_3$ transitions, respectively (Fig. S3a†).[14] The excitation spectrum of **1** monitored around the peak of the intense $^5D_4 \rightarrow {}^7F_5$ transition of the Tb(III) ion shows a broadband between 250 and 400 nm with a maximum at approximately 310 nm, which could be assigned to the π–π* electronic transition of the H_2PIP ligands.

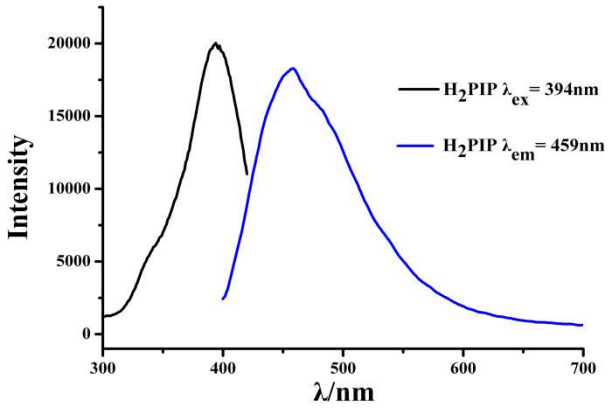

Fig. 3 Solid-state excitation and emission spectra for H_2PIP ligand at room temperature

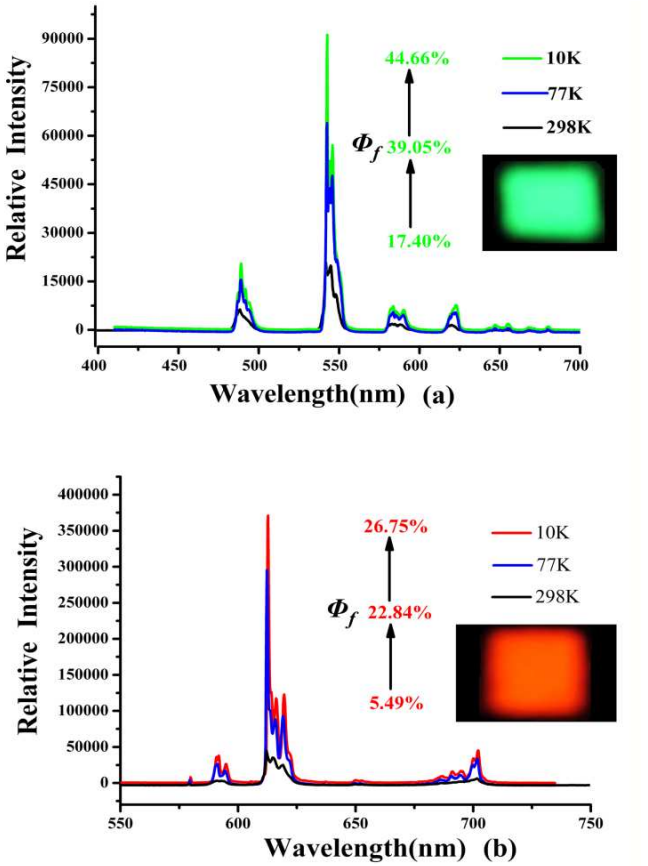

Fig. 4 Relative emission spectra of **1** (a) and **2** (b) with the variation of their fluorescent quantum yields collected in the solid state at 10, 77 and 298 K. Inset: fluorescent image of the green and red fluorescence **1** and **2** at 298 K.

As for **2**, the characteristic emissions of Eu(III) are observed in the range of 570–720 nm when excited at 338 nm. The typical emission peaks were associated with the 4f→4f transitions of the $^5D_0$ excited state of Eu(III) to its low-lying ^7F_J (J = 0, 1, 2, 3 and 4) levels (Fig. S3b†). The fluorescent intensity ratio of $^5D_0 \rightarrow {}^7F_2$ to $^5D_0 \rightarrow {}^7F_1$ transition reflects the information of the structure, such as the environments of the Eu(III) ions.[15] In addition, the intensity of $^5D_0 \rightarrow {}^7F_2$ transition is much stronger than that of $^5D_0 \rightarrow {}^7F_1$ transition.

The quantum yields of **1** and **2** were measured at 298, 77 and 10 K at the same excitation wavelength. As shown in Fig. 4, the quantum yields are 17.40% (298 K), 39.05% (77 K) and 44.66% (10 K) at λ_{ex} = 310 nm for **1** and 5.49% (298 K), 22.84% (77 K) and 26.75% (10 K) at λ_{ex} = 338 nm for **2**, respectively. The luminescence lifetimes of **1** and **2** were also obtained at 298, 77 and 10 K under the same excitation wavelengths (Table S4†). The corresponding lifetimes for **1** are τ_1 = 0.6935 (85.04%) ms and τ_2 = 0.1876 (14.96%) ms at 298 K; τ_1 = 0.9778 (93.43%) ms and τ_2 = 0.3116 (6.57%) ms at 77 K and τ_1 = 1.0000 (100%) ms at 10 K, respectively. While the lifetimes for **2** are τ_1 = 0.7653 (67.18%) ms and τ_2 = 0.3264 (32.82%) ms at 298 K; τ_1 = 1.086 (81.36%) ms and τ_2 = 0.3480 (18.64%) ms at 77 K and τ_1 = 1.185 (96.03%) ms and τ_2 = 0.372 (3.97%) ms at 10 K, respectively.

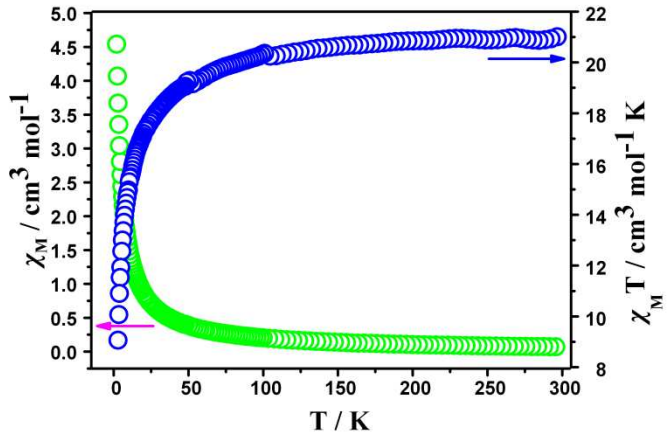

Fig. 5 Temperature dependence of χ_m and χ_mT values for **1**.

The luminescence curves are determined by monitoring $^5D_4 \rightarrow {}^7F_5$ line excited at 310 nm and $^5D_0 \rightarrow {}^7F_2$ line excited at 338 nm, respectively. It is obvious that the luminescent quantum yields and the lifetimes have similar temperature dependent behavior, revealing the absence of thermally activation and deactivation processes and further confirming the conclusion that the H_2PIP ligand is a good candidate to serve as ''antenna'' for Ln-Cps.[16]

Magnetic properties

Variable-temperature magnetic susceptibility measurement for **1** has been carried out in an applied magnetic field of 1000 Oe over the temperature range of 300−2 K. The plots of χ_mT and χ_m *versus* T are shown in Fig. 5, the χ_mT value is 21.12 cm^3 K mol^{-1} at room temperature, which is close to that expected for two independent Tb(III) ions (χ_mT = 23.65 cm^3 K mol^{-1} and g = 3/2, $^7F_6$).[17] Upon cooling, the χ_mT value decreases smoothly to reach the minimum value of 9.06 cm^3 K mol^{-1} at 2 K. This feature indicates the anti-ferromagnetic interactions between the Tb(III) ions. Above 10 K, the magnetic data was fitted by Curie-Weiss equation to give a Curie constant C = 21.28 cm^3 mol^{-1} and Weiss temperature θ = −4.59 K (Fig. S4†). The negative θ value also indicates the presence of anti-ferromagnetic interactions between the Tb(III) ions.

Conclusions

In summary, two novel 3D lanthanide supramolecular coordination polymers with lanthanide paddle wheel SBUs have been successfully synthesized and structurally characterized. They are isomorphic and both display a 2D layered structure, which is extended into a 3D supramolecular architecture by hydrogen bond interactions. They exhibit strong green and red fluorescent emissions respectively in the visible region at 10 K with moderate luminescence quantum yields and long luminescence lifetimes. Variable-temperature magnetic susceptibility measurement reveals an anti-ferromagnetic coupling between the Tb(III) ions in **1**.

Acknowledgments

This work was supported by National Basic Research Program of China (973 Program, 2012CB821702), the National Natural Science Foundation of China (21233009 and 21173221) and the

State Key Laboratory of Structural Chemistry, Fujian Institute of Research on the Structure of Matter, Chinese Academy of Sciences for financial support.

Notes and references

[a] *State Key Laboratory of Structural Chemistry, Fujian Institute of Research on the Structure of Matter, Chinese Academy of Sciences, Fuzhou, Fujian 350002, P. R. China. E-mail: swdu@fjirsm.ac.cn; Fax: (+86) 591-83709470*

[b] *University of Chinese Academy of Sciences, Beijing 100039, P. R. China.*

†Electronic Supplementary Information (ESI) available: Synthesis, Crystallographic information, additional figures, IR, TGA and XRD pattern. CCDC: 874175 (for **1**). For ESI and crystallographic data in CIF or other electronnic format see DOI: 10.1039/b000000x/.

1 (a) M. D. Allendorf, C. A. Bauer, R. K. Bhakta and R. J. T. Houka, *Chem. Soc. Rev.,* 2009, **38**, 1330; (b) Y. J. Cui, Y. F. Yue, G. D. Qian and B. L. Chen., *Chem. Rev.*, 2012, **112**, 1126.

2 (a) M. Kurmoo., *Chem. Soc. Rev*., 2009, **38**, 1353; (b) A. J. Tasiopoulos, A. Vinslava, W. Wermsdorfer, K. A. Abboub and G. Christou., *Angew. Chem. Int. Ed.,* 2004, **43**, 2117; (c) Y. Liu, Z. Chen, J. Ren, X. Q. Zhao, P. Cheng and B. Zhao., *Inorg. Chem.,* 2012, **51**, 7433; (d) H. L. Sun, Z. M. Wang and S. Gao., *Coord. Chem. Rev.,* 2010, **254**, 1081.

3 (a) J. Rocha, L. D. Carlos, F. A. Almeida and P. D. Ananias., *Chem. Soc. Rev.,* 2011, **40**, 926; (b) J. G. Wang, C. C. Huang, X. H. Huang and D. S. Liu., *Cryst. Growth Des.,* 2008, **8**, 795; (c) M. O. Keeffe and O. M. Yaghi., *Chem. Rev.,* 2012, **112**, 675; (d) Q. P. Li, J. J. Qian, C. B. Tian, P. Lin, Z. Z. He, N. Wang, J. N. Shen, H. B. Zhang, T. Chu, Y. Yang, L. P. Xue and S. W. Du, *Dalton Trans.*, 2014, **43**, 3238; (d) H. M. Yang, X. L. Song, T. L. Yang, Z. H. Liang, C. M. Fan and X. G. Hao., *RSC Adv.*, 2014, **4**, 15720.

4 (a) M. Li, D. Li, M. O'Keeffe and O. M. Yaghi., *Chem. Rev.*, 2014, **114**, 1343; (b) H. B. Zhang, Y. Peng , X. C. Shan, C. B. Tian, P. Lin and S. W. Du., *Inorg. Chem. Commun*., 2011, **14**, 1165; (c) T. R. Cook, Y. R. Zheng and P. J. Stang., *Chem. Rev.*, 2013, **113**, 734.

5 (a) B. L. Chen, L. B. Wang and G. D. Qian., *Angew. Chem. Int. Ed.* 2009, **48**, 500; (b) Y. H. Zhao, Z. M. Su, Y. M. Fu, K. Z. Shao, P. Li, Y. Wang, X. R. Hao, D. X. Zhu and S. D. Liu., *Polyhedron.,* 2008, **27**, 583; (c) J. L. Yi, Z. Y. Fu and S. J. Liao., *J. Coord. Chem.,* 2009, **14**, 2290; (d) Y. Y. Lv, Y. Qi, L. X. Sun, F. Luo, Y. X. Che and J. M. Zheng., *Eur. J. Inorg. Chem.*, 2010, 5592; (e) Y. T. Liu, Y. Q. Du, X. Wu, Z. P. Zheng, X. M. Lin, L. C. Zhu and Y. P. Cai., *CrystEngComm.,* 2014, DOI:10.1039/C4CE00417E.

6 (a) J. Huang, H. M. Li, J. Y. Zhang and C. Y. Su., *Inorg. Chim. Acta.*, 2012, **388** 16; (b) X. T. Rao, T. Song, B. L. Chen and G. D. Qian., *J. Am. Chem. Soc.*, 2013, **135**, 15559; (c) Q. F. Zhang, F. L. Hu, S. N. Wang and J. M. Dou., *Aust. J. Chem.* 2012, **65,** 524; (d) Y. G. Sun, J. Li, K. L. Li, Z. H. Xu, F. Ding, B. Y. Ren, S. J. Wang, L. X. You, G. Xiong and P. F. Smet., *CrystEngComm.,* 2014, **16**, 1777.

7 (a) C. P. Li, M. Du., *Chem. Commun.* 2011, **47**, 5958, (b) V. R. Pedireddi, S. Varughese., *Inorg. Chem.* 2004, **43**, 450. (c) L. L. Qu, Y. L. Zhu, Y. Z. Li, H. B. Du and X. Z. You., *Cryst. Growth Des.* 2011, **11**, 2444; (d) G. H. Xu, X. Y. He, J. Y. Lv, Z. G. Zhou, Z. Y. Du and Y. R. Xie., *Cryst. Growth Des.* 2012, **12**, 3619; (e) L. Luo, K. Chen, Q. Liu, Y. Lu, G. C. Lv, Y. Zhao and W. Y. Sun., *Cryst. Growth Des.* 2013, **13**, 2312.

8 (a) S. Q. Ma, D. Q. Yuan, X. Wang and H. C. Zhou, *Inorg. Chem*., 2009, **48**, 2072; (b) S. Q. Ma, X. Wang, D. Q. Yuan and H. C. Zhou, *Angew. Chem. Int. Ed.,* 2008, **47**, 4130; (c) S. K. Pandey and P. Kumar*., Eur. J. Org. Chem.,* 2007, 369.

9 (a) Z. Z. Li, L. Du, J. Zhou and Q. H. Zhao. *New J. Chem.*, 2013, **37**, 2473; (b) A. J. Zhou, J. D. Leng and M. L. Tong., *Dalton Trans.*, 2013, **42**, 9428; (c) J. Guo, D. Sun and D. F. Sun., *Cryst. Growth Des.,* 2012, **12**, 5649.

10 D. Zhu, J. Lv, X. J. L, S. Y. Gao, G. L. Li, F. X. Xiao and R. Cao., *Cryst. Growth Des.,* 2006, **8**, 1897.

11 *CrystalClear*, *version 1.36*, Molecular Structure Corp and Rigaku Corp., The Woodlands, TX, and Tokyo, Japan, 2000.

12 G. M. Sheldrick, *SHELXS 97*, *Program for Crystal Structure Solution*; University of Göttingen: Göttingen, Germany.

13 (a) Z. Z. Lin, J. H. Luo, M. C. Hong and R. Cao., J. *Solid State* Chem., 2004, **177**, 2494; (b) S. J. Li, D. L. Miao and S. W. Tong., *Acta Cryst*., 2011. **E67**, O1353; (c) Y. F. Zhang, Q. F. Zhang and D. Q. Wang., *Acta Cryst.*, 2010, **E66**, O2928; (d) A. D. Bond, N. Feeder and J. K. M. Sanders. *Acta Cryst*., 2001, **E57**, O869.

14 (a) H. B. Zhang, L. J. Zhou, J. Wei, Z. H. Li, P. Lin and S. W. Du., *J. Mater. Chem.,* 2012, **22**, 21210; (b) M. V. Lucky, S. Sivakumar, M. L. P. Reddy, A. K. Paul and S. Natarajan., *Cryst. Growth Des.,* 2011, **11**, 857.

15 (a) A. R. Ramya, M. L. P. Reddy and A. H. Cowley, *Inorg. Chem.* **2010**, *49*, 2407; (b) D. B. Ambili Raj, Biju Francis, M. L. P. Reddy, Rachel R. Butorac, Vincent M. Lynch and Alan H. Cowley., *Inorg. Chem*. 2010, **49**, 9055.

16 Z. H. Weng, D. C. Liu, Z. L. Chen, H. H. Zou, S. N. Qin and F. P. Liang., *Cryst. Growth. Des.,* 2009, **9**, 4163.

17 S. Y. Lin, G. F. Xu, L. Zhao, Y. N. Guo, Y. Guo and J. K. Tang., *Dalton Trans.*, 2011, **40**, 8213.